Global Sensitivity Analysis of Crop Yield and Transpiration from the FAO-AquaCrop Model for Dryland Environments

Yang Lu[a], Tendai P.Chibarabada[b], Matthew F.McCabe[c], Gabriëlle J.M. De Lannoy[d], Justin Sheffield[a]

[a] *Geography and Environment, University of Southampton, Southampton, United Kingdom*
[b] *Waternet, PO Box MP600, Mount Pleasant, Harare, Zimbabwe*
[c] *Division of Biological and Environmental Science and Engineering (BESE), King Abdullah University of Science and Technology, Thuwal, Saudi Arabia*
[d] *Department of Earth and Environmental Sciences, KU Leuven, Heverlee, Belgium*

Abstract

The application of crop models towards improved local scale prediction and precision management requires the identification and description of the major factors influencing model performance. Such efforts are particularly important for dryland areas which face rapid population growth and increasing constraints on water supplies. In this study, a global sensitivity analysis on crop yield and transpiration was performed for 49 parameters in the FAO-AquaCrop model (version 6.0) across three dryland farming areas with different climatic conditions. The Morris screening method and the variance-based Extended Fourier Amplitude Sensitivity Test (EFAST) method were used to evaluate the parameter sensitivities of several staple crops (maize, soybean or winter wheat) under dry, normal and wet scenarios. Results suggest that parameter sensitivities vary with the target model output (e.g., yield, transpiration) and the wetness condition. By synthesizing parameter sensitivities under different scenarios, the key parameters affecting model performance under both high and low water stress were identified for the three crops. Overall, factors relevant to root development tended to have large impacts under high water stress, while those controlling maximum canopy cover and senescence were more influential under low water stress. Parameter sensitivities were also shown to be stage-dependent from a day-by-day analysis of canopy cover and biomass simulations. Subsequent comparison with AquaCrop version 5.0 suggests that AquaCrop version 6.0 is less sensitive to uncertainties in soil properties.

Keywords: sensitivity analysis, dryland, AquaCrop, yield, transpiration

1. Introduction

Drylands are defined as areas with relatively low precipitation, long dry spells and frequent water scarce conditions (Wang et al., 2012). Drylands cover around 41% of the Earth's land surface (Reynolds et al., 2007), and are home to over 38% of the global population (Huang et al., 2016). Currently 90% of the dryland area population live in developing countries (Millennium Ecosystem Assessment, 2005), and exhibit a much higher growth rate compared to the global average (Wang et al., 2012). Combined, these issues highlight the need to identify key factors that impact crop growth to boost crop productivity.

Many crop models have been developed to simulate crop growth. Depending on the major driving factors, crop models are mainly categorized into carbon-driven, radiation-driven and water-driven models (Steduto, 2003). Among these models, the water-driven AquaCrop model is well suited for crop simulation in drylands, where water is a key limiting factor in crop production (Ran et al., 2020). The model was developed by the Food and Agriculture Organization (FAO) of the United Nations and mainly focuses on simulating the attainable biomass and crop yield in response to the available water (Steduto et al., 2009). Previous studies have generally suggested satisfactory model performance under multiple environmental conditions (Mabhaudhi et al., 2014; Bello and Walker, 2017; Akumaga et al., 2017; Mbangiwa et al., 2019; Adeboye et al., 2019; Xu et al., 2019; Sandhu and Irmak, 2019a,b; Chibarabada et al., 2020).

To determine the key influential factors within crop models, one approach is to perform sensitivity analysis (SA) (Pianosi et al., 2015). SA quantitatively evaluates the impact of uncertainties in the model input (e.g., parameters) on the model output (e.g., yield), and is instrumental in (i) understanding the interplay between modules and processes, (ii) identifying the high-impact and low-impact factors, and (iii) identifying imbalanced model structure, where model performance is dominated by a small number of parameters (Cariboni et al., 2007; Confalonieri et al., 2010a,b; Nossent et al., 2011; Vanuytrecht et al., 2014b; Pianosi et al., 2016). SA techniques have been applied to many crop models, such as the Water Accounting Rice Model (WARM) (Confalonieri et al., 2010a,b), the Simple Algorithm For Yield (SAFY) model (Silvestro et al., 2017b), the WOrld FOod STudies (WOFOST) model (Wang et al., 2013), the CoupModel (Wu et al., 2019), and the AquaCrop model (Vanuytrecht et al., 2014b; Silvestro et al., 2017b; Jin et al., 2018).

Overall, SA techniques can be categorized into local SA and global SA

(Saltelli et al., 2000a). Local SA examines the response of the model output to the variation of an input, while keeping the other inputs fixed. Local SA is easy to implement but may lead to unrealistic sensitivity assessment since the sensitivity of a specific input depends on the values of other inputs, which is particularly evident in non-linear models (Saltelli and Annoni, 2010). Global SA is more prevalent since it builds on the average response of the model output when all inputs are allowed to vary within a pre-defined range. Global SA is capable of capturing the non-linear model responses and the interactions between model inputs at the cost of larger computational burden (Cariboni et al., 2007; Saltelli and Annoni, 2010). Out of the many global SA methods, the screening methods and the variance-based methods are widely used (Iooss and Lemaître, 2015). The most commonly used screening approach is the Morris method (Morris, 1991), which is based on the computation of the average elementary effect of individual parameter changes on the model output (Vanuytrecht et al., 2014b). The Morris method is very effective in identifying a few influential factors among a large set of parameters. The variance-based methods calculate the first and higher order sensitivity indices based on decomposing the output variance, and are more computationally demanding as a result of the large number of model evaluations required (Confalonieri et al., 2010a). Frequently used methods include the Sobol' method (Sobol, 1993), the Fourier Amplitude Sensitivity Test (FAST) (Cukier et al., 1978) and the Extended FAST (EFAST) (Saltelli et al., 1999), distinguished by the way the parameter space is sampled.

Though a number of SA studies have been performed for AquaCrop (Vanuytrecht et al., 2014b; Silvestro et al., 2017b; Jin et al., 2018), some limitations are yet to be addressed:

(i) No studies so far have focused specifically on drylands. Since the SA results depend on the environmental conditions such as climate types and dry-normal-wet conditions (Vanuytrecht et al., 2014b; Liu et al., 2019), the SA results derived in other regions are not directly transferable to drylands.

(ii) Most SA studies focused solely on crop yield, while the sensitivity of crop transpiration, which forms the basis for yield production (Liu et al., 2009; Lin, 2010) and has significant importance for irrigation management (Qiu et al., 2019), land-atmosphere interaction (Williams and Torn, 2015) and the water cycle (Schlesinger and Jasechko, 2014), has not been explored.

(iii) Most SA studies were based on one typical growing season under each scenario, which essentially neglects the potential impact of variation in the temporal distribution of precipitation.

(iv) Most SA studies evaluate the output sensitivity to soil parameters by directly adding perturbations to soil hydraulic properties, which may lead to unrealistic or even contradictory combinations of different soil properties.

(v) The vast majority of SA studies derive constant parameter sensitivities of the final model outputs, while the sensitivity dynamics at different phenological stages remains largely unexplored apart from a couple of recent studies (Jin et al., 2018; Guo et al., 2019).

(vi) In the recent model update (version 6.0), the simulation under very dry environments was improved. This may lead to different sensitivity evaluations in drylands compared to earlier model versions (5.0 or older).

In this study, a global SA was conducted for the AquaCrop model (version 6.0) with a specific focus on drylands. Three dryland farming areas with different climatic conditions in the United States, Zambia and China were selected, and the SA was performed for crop yield and transpiration of several staple crops (maize, soybean and winter wheat) separately. The objectives of this study were (1) to distinguish influential/non-influential parameters on crop yield and transpiration over drylands, and (2) to identify parameter sensitivities for the three crops under diverse climatic conditions, and (3) to derive parameter sensitivity dynamics over the growing season. Findings from this study can provide insight on key AquaCrop parameter calibration, future model improvement and data assimilation applications.

2. Materials and Methods

The Morris method was first used to screen out parameters with marginal effects, and then the EFAST method was implemented to quantify both the first and higher order parameter sensitivities. Three scenarios (dry, normal and wet) were determined based on the historical meteorological data, and 7 different growing seasons were simulated for each scenario to address the differences within the same scenario. Soil properties were generated using pedotransfer equations from perturbed texture data to derive consistent soil properties. Further, the temporal dynamics of parameter influence on canopy cover and crop biomass, which are often used in agricultural data assimilation, were evaluated during the growing season. Finally, the whole experiment was rerun using AquaCrop version 5.0 to assess the parameter sensitivity difference between the two model versions.

2.1. The AquaCrop Model

The AquaCrop model (Steduto et al., 2009; Raes et al., 2009) is a generic water-driven model evolved from the crop evapotranspiration and yield reduction approach proposed by Doorenbos and Kassam (1979). When developing AquaCrop, the FAO aimed for a simple model that was robust and practitioner-oriented (Steduto et al., 2009). In AquaCrop, the crop yield is estimated in the following procedures: (i) simulate crop canopy development indicated by the fractional canopy cover (CC); (ii) calculate crop transpiration as a function of CC, the reference evapotranspiration (ET_0) and water stress; (iii) calculate crop biomass from transpiration; and (iv) calculate yield from crop biomass (Steduto et al., 2009; Raes et al., 2009; Hsiao et al., 2009; Vanuytrecht et al., 2014a). The dry above-ground biomass (B) and crop yield (Y) are determined by

$$B = wp^* \cdot \sum \frac{Tr}{ET_0} \tag{1}$$

$$Y = B \cdot HI \tag{2}$$

where Tr is crop transpiration, wp^* is the water productivity normalized for atmospheric evaporative demand and CO_2 concentration, and HI is the crop-specific harvest index. The normalized water productivity was shown to not vary significantly within genotypes of the same species (Steduto et al., 2007) and can be assumed conservative. If the crop encounters stress during flowering or yield formation, HI is adjusted (Vanuytrecht et al., 2014a).

Expressing the foliage development using the CC instead of the commonly used leaf area index (LAI) is a distinctive feature of AquaCrop, which introduces significant simplification in the model simulation (Steduto et al., 2009; Raes et al., 2018c). The model simulations can be performed based on both thermal time (growing degree day (GDD)) and calendar time at daily time steps. The forcing data required are precipitation, minimum and maximum temperature and ET_0. In this study an open-source version of AquaCrop (Foster et al., 2017) based on the AquaCrop v6.0 was adopted. A total of 49 parameters (listed in Table 1) were considered in the sensitivity analysis.

Table 1: AquaCrop parameters evaluated in this study.

Parameter	Description	Unit
Crop Development		
tb	base temperature below which crop growth does not occur	°C
tu	upper temperature above which crop growth does not occur	°C
ccs	soil surface covered by an individual seedling at 90% emergence	cm^2
den	plant population per hectare	-
eme	time from sowing to emergence	GDD's
cgc	canopy growth coefficient	Fraction GDD^{-1}
ccx	maximum fractional canopy cover size	-
sen	time from emergence to start of canopy senescence	GDD's
cdc	canopy decline coefficient	Fraction GDD^{-1}

mat	time from emergence to physiological maturity	GDD's
flo	time from emergence to flowering	GDD's
flolen	duration of flowering	GDD's
rtm	minimum effective rooting depth	m
rtx	maximum effective rooting depth	m
rtshp	shape factor describing root zone expansion	-
root	time from sowing to maximum root development	GDD's
rtexup	maximum water extraction at the top of the root zone	m^3/m^3/day
rtexlw	maximum water extraction at the bottom of the root zone	m^3/m^3/day
Crop Transpiration		
kc	crop coefficient when canopy is complete but prior to senescence	-
kcdcl	decline of crop coefficient due to ageing of the canopy	% day^{-1}
Biomass and Yield		
wp^*	water productivity normalized for ET_0 and CO_2	g/m^2
wpy	adjustment of wp^* in yield formation stage	% of wp^*
hi	reference harvest index	-
hipsflo	possible increase of *hi* due to water stress before flowering	%

exc	excess of potential fruits	%
hipsveg	coefficient describing positive impact of restricted vegetative growth during yield formation on *hi*	-
hingsto	coefficient describing negative impact of stomatal closure growth during yield formation on *hi*	-
hinc	maximum possible increase in *hi* above reference value	%
hilen	duration of yield formation	GDD's
Water and Temperature Stress		
anaer	water deficit below saturation at which aeration stress begins to occur	%
polmn	minimum temperature below which pollination begins to fail	°C
polmx	maximum temperature above which pollination begins to fail	°C
stbio	minimum number of GDD's required for full biomass production	GDD's day^{-1}
prtshp	shape factor describing the effects of water stress on root expansion	-
pexup	upper soil water depletion threshold for water stress on canopy expansion	-
psto	upper soil water depletion threshold for water stress on stomatal control	-

psen	upper soil water depletion threshold for water stress on canopy senescence	-
ppol	upper soil water depletion threshold for water stress on pollination	-
pexlw	lower soil water depletion threshold for water stress on canopy expansion	-
pexshp	shape factor for water stress effects on canopy expansion	-
pstoshp	shape factor for water stress effects on stomatal control	-
psenshp	shape factor for water stress effects on canopy senescence	-
Soil		
evardc	effect of canopy cover on reducing soil evaporation in late season stage	%
cn	curve number	-
kex	maximum soil evaporation coefficient	-
rew	readily evaporable water	mm
sand	sand fraction	%
clay	clay fraction	%
Management		
pdate	day of sowing	-

2.2. Data

The daily precipitation as well as minimum and maximum temperature data are from the Princeton Global Forcing (PGF) dataset v3 (Sheffield et al., 2006). This dataset is constructed by combining a suite of observation-based datasets with the National Centers for Environmental Prediction-National Center for Atmospheric Research (NCEP − NCAR) reanalysis data, and provides global daily meteorological data from 1948 to 2016 at 0.25° resolution. Daily ET_0 data were calculated using the FAO Penman-Monteith (FAO-PM) method (Allen et al., 1998) from solar radiation, air temperature, wind speed and specific humidity data from the PGF dataset.

2.3. Experimental Sites

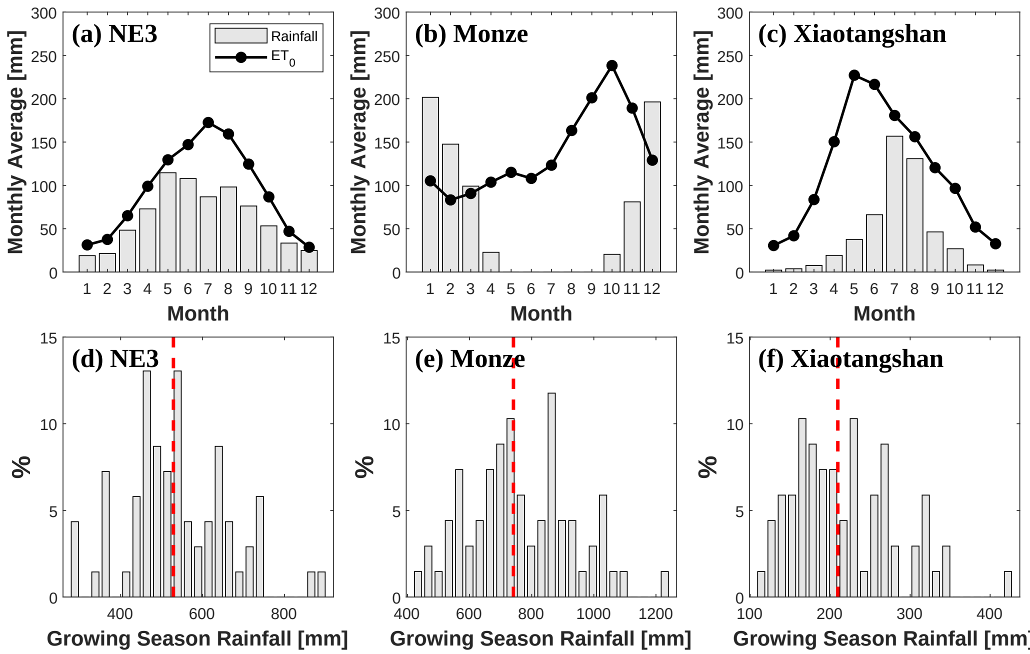

Figure 1: The monthly average rainfall and reference evapotranspiration (a-c) and histogram of growing season rainfall during 1948 and 2016 (d-f) at the experimental sites. The red dashed lines indicate median values.

Three experimental sites with distinct climatic and aridity conditions were selected. The monthly average rainfall and ET_0 as well as the histogram of growing season rainfall are shown in Figure 1. The first site NE3 (41.18° N, 96.44° W, alt. 363 m) is located near Mead in eastern Nebraska, United States. The field covers an area of 65.4 ha (Verma et al., 2005), and the soil is mostly silt loam and silty clay loam (Foolad et al., 2017). The mean daily maximum temperature is 17.1 °C, and the mean daily minimum temperature is 4.4 °C. The region has a continental semi-arid climate, and precipitation mainly occurs between April and September. Maize (*Zea mays*

L.) and soybean (*Glycine max(L) Merr*) were rotationally grown under rain-fed conditions during the growing season from May to October (Foolad et al., 2017). In each growing season, a different hybrid/cultivar is planted.

The second site Monze (16.24° S, 27.44° E, alt. 1103 m) is located in southern Zambia, south of Lusaka. The mean daily maximum temperature is 29.6 °C, and the mean daily minimum temperature is 15.4 °C. The region has a sub-tropical climate and features a wet season and a dry season. Almost all precipitation occurs between mid-November and April, and the inter-annual variability is very evident (Figure 1e). The growing season is from October to April of the following year. Maize (*Zea mays L.*) is the principle crop in this area and is planted under rain-fed condition (Thierfelder and Wall, 2009).

The third site Xiaotangshan (40.17° N, 116.43° E, alt. 57 m) is located in northern China near Beijing. The mean daily maximum temperature is 18.6 °C, and the mean daily minimum temperature is 7.0 °C. This is the major winter wheat (*Triticum aestivum L.*) growing region in China with a continental climate, featuring a cold dry winter and a hot wet summer. The growing season is from September to June of the following year, while precipitation mainly occurs between April to September (Silvestro et al., 2017b).

2.4. The Morris Method

The Morris method (Morris, 1991) is a commonly used screening method. It attempts to globally aggregate local sensitivity information (first-order derivatives) across the parameter space (Razavi and Gupta, 2015). For the ith parameter x_i, the elementary effect (d_i) of a small value change on the model output is calculated by

$$d_i = \frac{y(x_1, \ldots, x_{i-1}, x_i + \Delta_i, x_{i+1}, \ldots, x_n) - y(x_1, \ldots, x_{i-1}, x_i, x_{i+1}, \ldots, x_n)}{\Delta_i} \tag{3}$$

where $X = (x_1, ..., x_n)$ is the n-dimensional parameter vector considered in the sensitivity test, $y(X)$ is the model output, Δ_i is a pre-determined multiple of $1/(p-1)$, and p is the number of levels corresponding to quantiles of the parameter distribution.

The method samples parameter values from the n-dimensional p-level hyperspace and calculates the mean (μ) and standard deviation (σ) of all elementary effects. Following Campolongo et al. (2007), the mean of the absolute values of the elementary effects (μ^*) was used in this study to account for potential model non-monotonic behaviour. The parameters μ^* and σ are calculated over different trajectories, which indicates the intensity with which the parameter space is explored. Large μ^* values indicate higher influence on the model output and large σ values indicate more interactions with other parameters or the non-linear model response. The main advantage of the Morris method is its low computational demand, which makes it particularly useful in identifying a subset of influential factors among a large set of parameters.

2.5. The EFAST Method

The EFAST method (Saltelli et al., 1999) is a widely-used variance-based SA method which is based on decomposing the total variance of model output into the first-order and higher-order contributions of parameter variation:

$$V(y) = \sum_{i=1}^{k} V_i + \sum_{i \leq j \leq k}^{k} V_{ij} + \cdots + \sum_{i \leq \ldots \leq k}^{k} V_{i \ldots k} \tag{4}$$

where k is the number of parameters analysed, $V(y)$ is the total output variance, V_i is the main effect of the parameter x_i, and V_{ij} to $V_{i \ldots n}$ are the contributions of second to higher-order interactions among parameters to the output variance. $V(i)$ is calculated by

$$V_i = V[E(y|x_i)] \tag{5}$$

where $E(y|x_i)$ is the expectation of model output conditional on a fixed x_i value.

In variance-based methods, two sensitivity indices are calculated: the main effect sensitivity index (S_i) of x_i:

$$S_i = \frac{V_i}{V(y)} \tag{6}$$

and the total sensitivity index (ST_i):

$$ST_i = 1 - \frac{V_{-i}}{V(y)} \tag{7}$$

where V_{-i} is the estimated conditional variance of model output except for x_i. S_i measures only the contribution of the input parameter on the output variance, while ST_i also accounts for the interactions with other parameters.

The EFAST method distinguishes itself from other variance-based methods in the search curve used to explore the parameter hyperspace:

$$x_i = 0.5 + \frac{1}{\pi} \cdot arcsin[sin(\omega_i s + \phi_i)] \tag{8}$$

where ω_i is a frequency associated to x_i, s is a scalable value ranges between $-\pi$ and π, and ϕ_i indicates the starting point of the search curve. The total number of model runs (N) per growing season per experimental site is

$$N = k * N_r * (2 * M * \omega_{max} + 1) \tag{9}$$

where M is maximum number of Fourier coefficients that may be retained in calculating the partial variances without interferences between the assigned frequencies (set to 4), ω_{max} is the maxima in the set of ω_i frequencies (49 in this case), and N_r is the number of search curves indicating the times the EFAST algorithm is repeated with a random phase shift each time (N_r=25).

2.6. Experiment Set-up

For each experimental site, the dry, normal and wet scenarios were determined using a percentile-based approach. The growing season precipitation was calculated based on the PGF data between 1948 and 2016 (69 years in total) and sorted in the ascending order. The dry, normal and wet scenarios were defined as the 7 growing seasons within the 0-10%, 45%-55%, and 90%-100% percentiles. A total of 21 growing seasons were simulated for each site-crop combination. The growing season precipitation under each scenario is summarized in Table 2.

The simulations were run under rain-fed conditions, and fertility stress was not evaluated in this experiment. A five-month spin-up period was simulated prior to the the start of each growing season individually, using the actual meteorological forcing data to eliminate the influence of soil moisture initialization uncertainties. Soil properties (field capacity, saturated soil

Table 2: Growing season precipitation (mm) in the selected scenarios at the experimental sites.

	Dry Scenario			**Normal Scenario**			**Wet Scenario**		
Site	Min	Max	Median	Min	Max	Median	Min	Max	Median
NE3	325	398	367	529	553	538	730	932	775
Monze	418	546	517	727	778	737	1027	1245	1038
Xiaotangshan	107	142	128	201	213	210	320	429	338

moisture, wilting point and saturated hydraulic conductivity) were derived from soil texture data (Saxton and Rawls, 2006) to keep the properties consistent. The parameter ranges are provided in the supplementary materials.

The SA was performed for each experimental site using crop yield and total transpiration as the target output, respectively. The Morris method was first implemented, and parameters with μ^* above a given threshold were defined as the influential parameters. The thresholds used for crop yield and total transpiration were 0.25 $\mathrm{t \cdot ha^{-1}}$ and 10 mm. The yield threshold was taken after Vanuytrecht et al. (2014b), and the transpiration threshold was determined based on expert knowledge of the study area. In this study, 500 trajectories were used for each Morris SA, which resulted in 25,000 model runs per site-crop combination per growing season. The influential parameters were then analysed using the EFAST method. The number of influential parameters depends on the site and scenario. The simulations required per site-crop combination per growing season were between 108,075 and 284,925 for crop yield analysis, and between 68,775 and 216,150 for total transpiration analysis. Convergence tests using different sensitivity analysis configurations suggested that the results from the Morris and the EFAST methods were stable.

3. Results

3.1. Analysis using the Morris Method

3.1.1. Morris Results for Crop Yield

The mean elementary effect (μ^*) and standard deviation (σ) for crop yield from the Morris analysis are shown in Figure 2. The results for different site-crop-scenario combinations are plotted in sub-graphs. The three parameters with the largest μ^* are annotated. The standard deviations of μ^* and σ estimates from the 7 growing seasons in each scenario are also plotted using horizontal and vertical error bars.

At the NE3 site, both maize and soybean were modelled using the same forcing data for each scenario. In the SA for maize (Figure 2a-c), the major influential factors demonstrate some similarities among different scenarios. The most influential factors are *rtx*, *sen*, *hilen*, *wpy* and *ccx*. *hilen* determines the length of yield formation, while other factors are closely related either to the crop's ability to make use of the water resources (*rtx*, *sen*, *ccx*) or to the efficiency to produce biomass per unit of water (*wpy*). For soybean (Figure 2d-f), the analysis displays some similarities with that for maize, with *rtx* being the most influential factor for the dry scenario and *sen* gaining importance from the dry to the wet scenario. An evident difference is the much larger influence of wp^*. In addition, *hilen* is not a major influential factor under any scenario. The Morris results for maize at the Monze site (Figure 2g-i) are similar among the three scenarios. The most influential factors are *hilen*, *sen* and *flo*, followed by *wpy*, *mat*, *tb*, *ccx* and *cdc*, among which

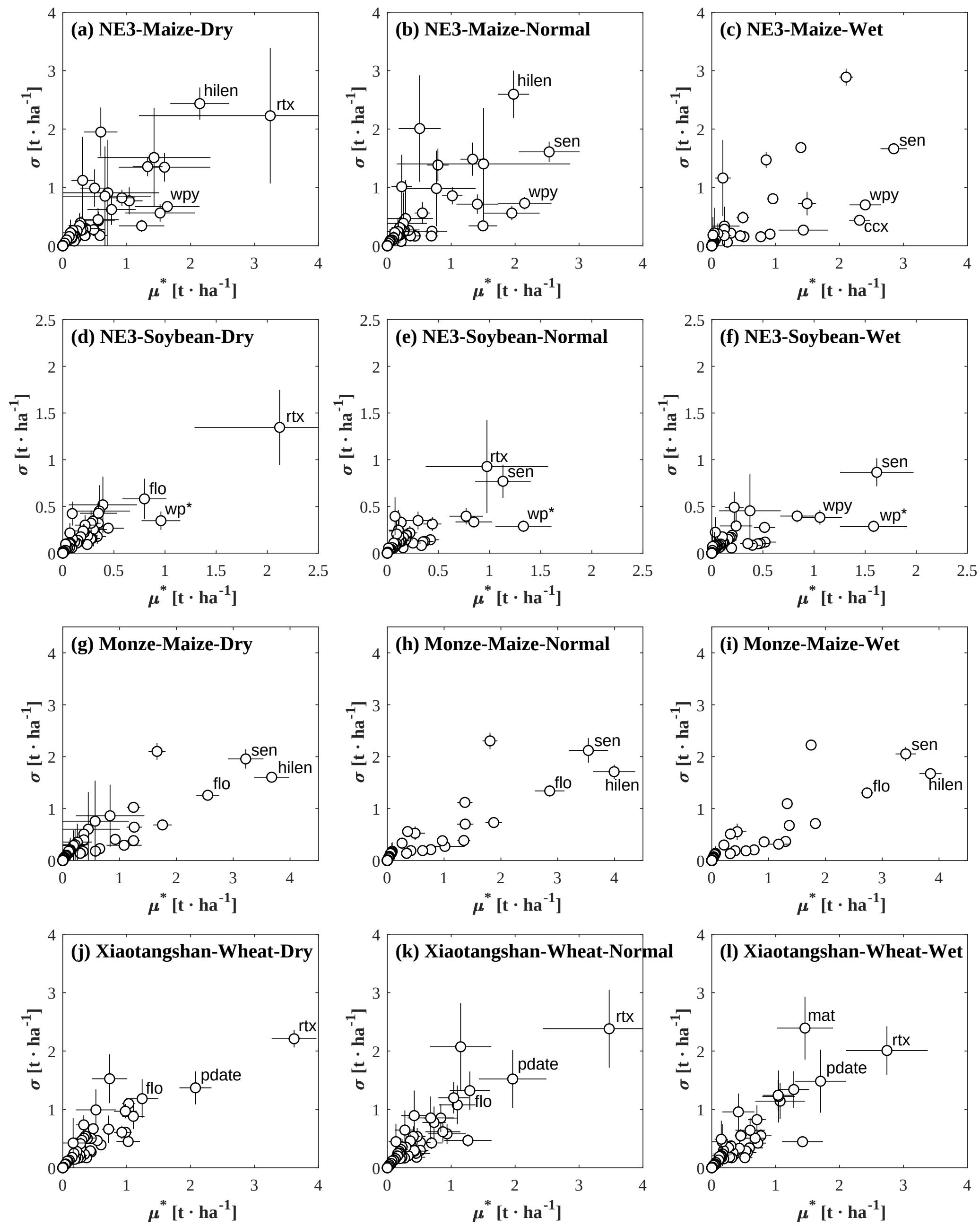

Figure 2: Mean elementary effect (μ^*) on crop yield and its standard deviation (σ) under different scenarios from the Morris analysis. The error bars indicate standard deviation of the metrics among the 7 growing seasons under each scenario.

many are related to the canopy growth or water productivity. The results are similar to those for maize at the NE3 site under the wet scenario, where the water stress is low. At the Xiaotangshan site (Figure 2j-l), the results are also similar under different scenarios. *rtx* has a much larger influence than other factors, and other influential factors include *pdate*, *flo*, *mat*, *tb* and wp^*, which relates to the relatively low growing season precipitation.

Following Vanuytrecht et al. (2014b), a threshold of 0.25 $\mathrm{t \cdot ha^{-1}}$ for μ^* was adopted to distinguish between the influential and non-influential parameters for crop yield. The number of influential parameters ranges between 11 and 29, depending on the experimental site and scenario. For all sites and crops, the dry scenario tends to have more influential parameters than the wet scenario. Factors with negligible influence ($\mu^* < 0.25\ \mathrm{t \cdot ha^{-1}}$) at all sites for all scenarios are *pexlw*, *pexup*, *hipsflo*, *stbio*, *cn*, *rtm*, *evardc*, *flolen*, *polmn*. In particular, the μ^* of *anaer*, *hinc*, *polmx* and *rew* is always zero.

3.1.2. Morris Results for Crop Transpiration

The Morris SA results using the total crop transpiration in the growing season as the target model output are displayed in Figure 3. For maize at the NE3 site (Figure 3a-c), *ccx* is a major influencing factor under all scenarios. Similar to the Morris results for maize yield, *rtx* has a much larger impact under the dry scenario, while the importance gradually decreases under the normal and wet scenarios. Under the dry and normal scenarios, large variations are seen among different growing seasons, indicated by the long error bars, which decrease dramatically under the wet scenario. This suggests that the factors' influence is steady under low water stress and is more growing season-specific under high to moderate water stress. For soybean (Figure

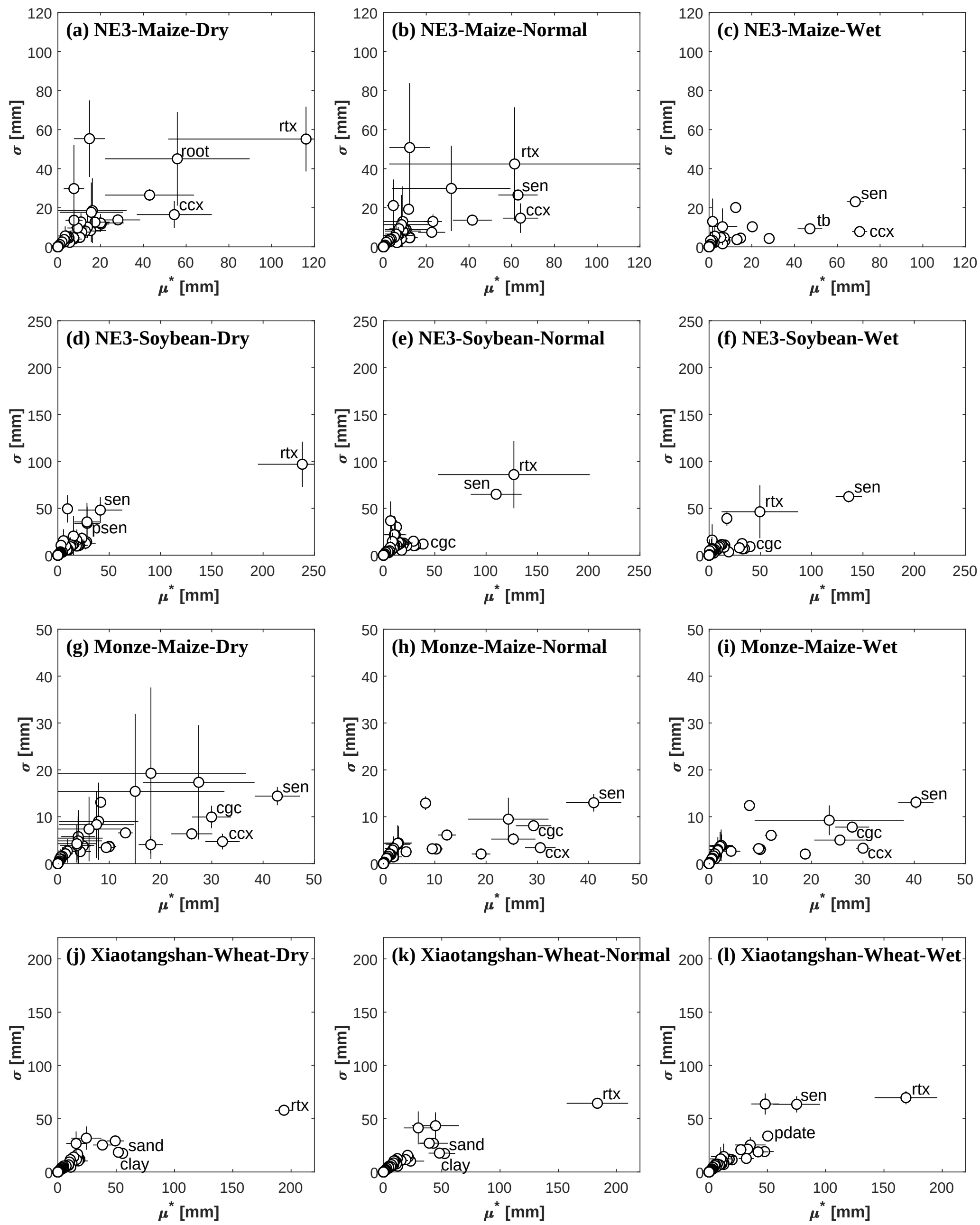

Figure 3: Mean elementary effect (μ^*) on total transpiration and its standard deviation (σ) under different scenarios from the Morris analysis.

3d-f), the influence is dominated by rtx under the dry scenario, while other factors have much smaller influence. Under the wet scenario, rtx ranks second with a much smaller μ^*, and sen becomes the most influential factor. At the Monze site, the influential factors for total transpiration are also similar under different scenarios (Figure 3g-i). As a result of the relative abundance of precipitation, the major influential factors are sen, ccx, and cgc, followed by $pdate$, tb, kc and cdc, which are all closely related to canopy development. At the Xiaotangshan site, the Morris results also demonstrate similar patterns under different scenarios (Figure 3j-l). The influence on total transpiration is dominated by rtx, which again highlights the severe water stress at this site. Under the dry and normal scenarios, rtx is followed by $clay$ and $sand$, which may relate to their impact on soil hydraulic properties (Saxton and Rawls, 2006).

A threshold of 10 mm for μ^* was used to identify influential factors for total transpiration. The number of influential factors varies from 7 to 22, depending on the experimental site and scenario. Factors with non-zero but negligible influence ($0 < \mu^* < 10$ mm) at all sites for all scenarios are $flolen$, $pexup$, $rtexup$, $pstoshp$, rtm, $anaer$, $evardc$. Many factors have zero influence on the total transpiration under all conditions, including wp^*, wpy, hi, $hipsflo$, exc, $hipsveg$, $hingsto$, $hinc$, $hilen$, $polmn$, $polmx$, $ppol$ and rew.

3.1.3. Comparison of the Morris SA Results

The Morris results for crop yield and for total transpiration both indicate that the model responds differently to parameter variations under different scenarios. Under high to moderate water stress, crops with deeper roots can make better use of the limited soil water for survival (Koevoets et al., 2016;

Fang et al., 2017; Wasaya et al., 2018), rendering root-related parameters more influential than others. In contrast, the maximum coverage that the crop canopy can reach, along with the canopy growth and decline rates, are more important when the water supply is abundant. Consequently, different influential factors were identified under different environmental conditions.

Despite the similarities between Morris results for crop yield and for total transpiration, some differences are noteworthy. Some factors that prove influential on crop yield have no influence at all on the total transpiration, such as *hilen*, wp^* and *wpy*. This is expected as the parameters are involved in the biomass accumulation and yield formation processes, which are less relevant to crop transpiration processes. Aside from the stark disparity, the differences in the influence magnitude of some factors (e.g., *mat*, *sand*, *clay*) are also evident. This suggests that the key factors to be considered also depend on the target model output of interest.

Although the Morris analysis does not quantify the impact of parameter interactions, the relatively high σ indicates strong interactions among parameters and/or non-linear model behaviour. The long horizontal and vertical error bars of μ^* and σ imply that even within one scenario, the difference in the temporal distribution of precipitation can play an important role in the impact of parameters.

3.2. Analysis using the EFAST Method

3.2.1. EFAST Results for Crop Yield

Based on the SA results from the Morris method, parameters with $\mu^* > 0.25\ \mathrm{t \cdot ha^{-1}}$ on crop yield were further analysed using the EFAST method. The first-order (main) sensitivity indices (S_i) and the total (S_i plus parameter interactions) sensitivity indices (ST_i) were quantified. For maize at the NE3 site (Figure 4a-c), the EFAST method confirms that *rtx* and *sen* are the most influential factors on crop yield under the dry and wet scenarios, respectively. The parameter rankings are similar to those from the Morris screening analysis, confirming the validity of the Morris method. Interactions among parameters are evident, highlighted by the large difference between ST_i and S_i, particularly under the dry and normal scenarios. The results are also consistent with the Morris analysis for soybean (Figure 4d-f). Unlike the maize experiment, where many factors have non-negligible impact on crop yield, the soybean yield is dominated by the influence of *rtx* under the dry scenario. The *rtx* alone (S_i) contributes to around 50% of the variance in soybean yield under the dry scenario. However, the sensitivity index of *rtx* drops to around 20% under the normal scenario and to almost zero under the wet scenario, while *sen* and wp^* become the most influential parameters. Combined, *sen* and wp^* contribute to over 40% and 60% of the yield variance under the normal and wet scenarios, respectively.

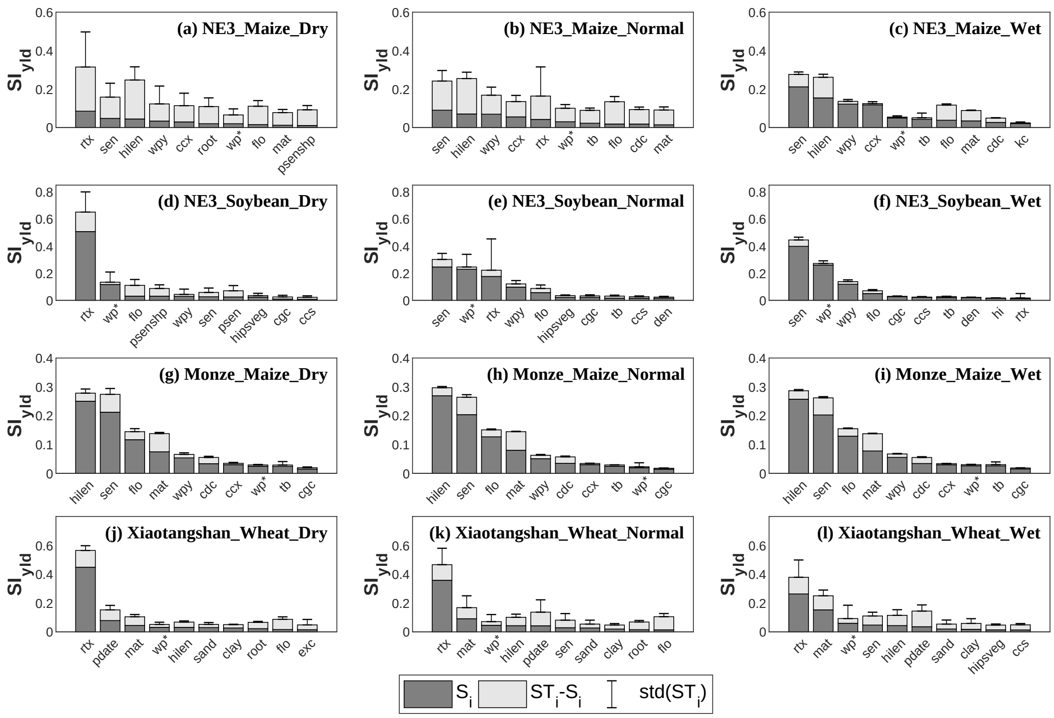

Figure 4: The sensitivity indices for crop yield ($\mathrm{SI}_{\mathrm{yld}}$) using the EFAST method. S_i indicates the first-order sensitivity, $ST_i - S_i$ represents parameter interactions, and the error bars are a measure of the difference between different growing seasons. The parameters are ranked in descending order of S_i, and only the 10 most influential parameters are plotted.

At the Monze site (Figure 4g-i), the factor rankings and the sensitivity magnitudes are similar under different scenarios. Many factors have considerable impacts on the maize yield, while the largest three factors ($hilen$, sen, flo) contribute to over 50% of the yield variance. At the Xiaotangshan site (Figure 4j-l), rtx has a dominant impact on the winter wheat yield under the dry scenario, which gradually decreases under the normal and wet scenarios, while the decrease of water stress leads to an increased influence of mat under the normal and wet scenarios. This is consistent with the findings in Silvestro et al. (2017b) that *rtx* has a larger impact in the dry year while *mat* has a larger impact in the wet year.

3.2.2. EFAST Results for Crop Transpiration

The parameters with $\mu^* > 10$ mm on crop transpiration based on the Morris method were further analysed using the EFAST method. For maize at the NE3 site (Figure 5a-c), the three scenarios show distinct features, and the factor rankings agree very well with the Morris results. Under the wet scenario, the parameter interactions are only marginal, and the crop transpiration is dominated by *ccx*, *sen* and *tb* with a combined S_i of over 80%. Different from the results for maize, the sensitivity of soybean transpiration at NE3 is dominated only by a limited number of parameters (Figure 5d-f). Under the dry scenario, the transpiration variance is almost entirely attributed to variations in *rtx*. Under the wet scenario, around 60% of the transpiration variance is attributed to the main effect of *sen*.

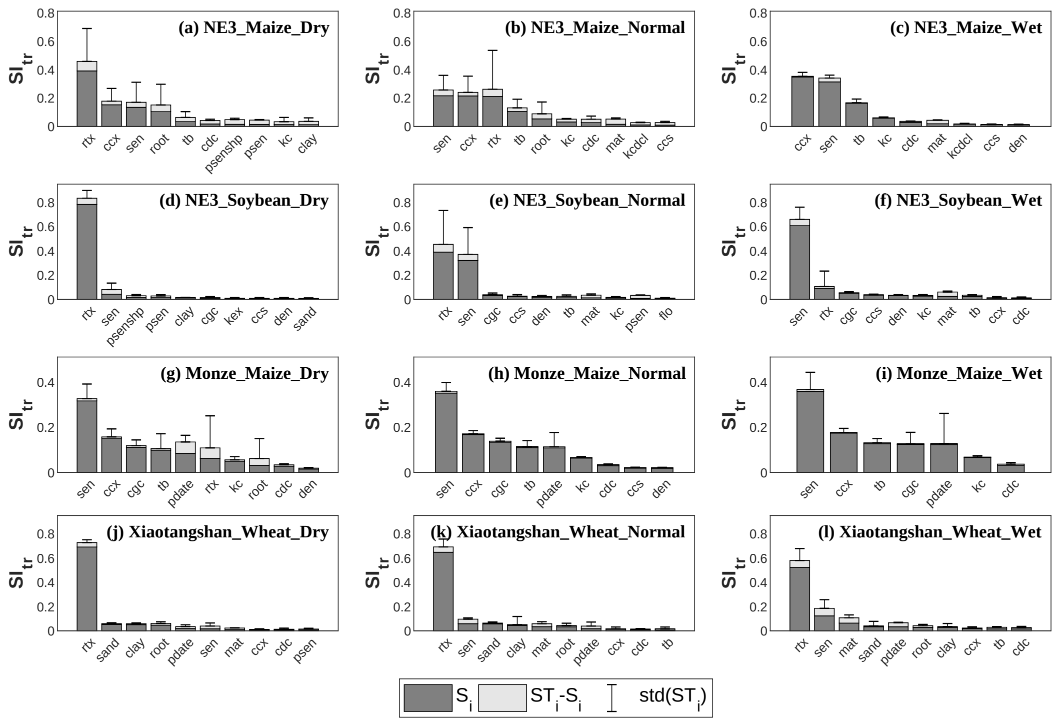

Figure 5: The sensitivity indices for crop transpiration ($\mathrm{SI}_{\mathrm{tr}}$) using the EFAST method.

At the Monze site (Figure 5g-i), the EFAST results confirm the similarity of parameter rankings under the three scenarios shown by the Morris results. The largest influential factor is *sen* which accounts for over 30% of the transpiration variance, followed by *ccx*, *cgc*, *tb* and *pdate*. Overall, the parameter interactions are relatively small. At the Xiaotangshan site (Figure 5j-l), the crop transpiration variance is mainly determined by *rtx*, which is consistent with the EFAST results for crop yield (Figure 4j-l). The influence comes almost entirely from the main effect, and the sensitivity index variations within one scenario are negligible.

3.3. Sensitivity Dynamics in the Growing Season

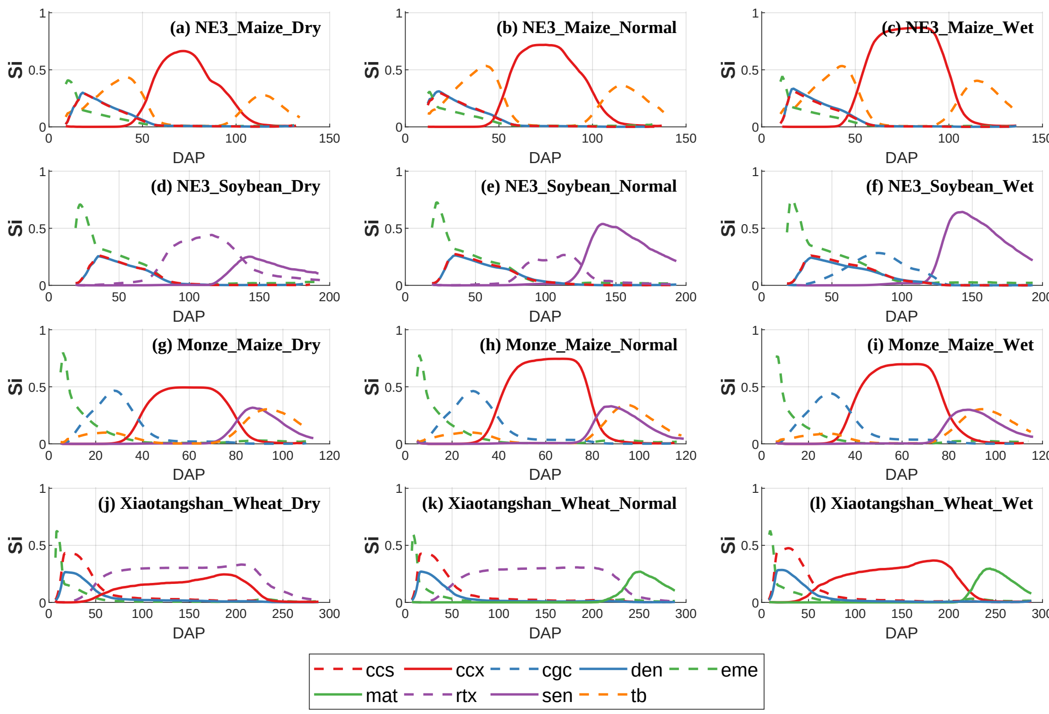

Figure 6: S_i time series of the five most influential factors on crop canopy cover throughout the growing season.

As the main eco-physiological processes of the crop vary with growth stage (Wang et al., 2013), the influence of parameters is expected to be stage-dependent. By replacing the model output (crop yield or total transpiration) in the sensitivity analysis with daily simulated CC and biomass, the temporal dynamics of the sensitivity indices during the growing season were derived. CC and biomass were selected because they were frequently used in agricultural data assimilation and have great potential to improve model performance by adjusting key model parameters through assimilation.

Figure 6 demonstrates the main sensitivity index S_i time series for CC with days after planting (DAP) for the five most influential parameters. Among all the site-crop-scenario combinations, eme is the only influential parameter on CC in common, which dominates the canopy growth in the initial days shortly after planting. The influence then decreases sharply to almost zero after the first one to two months. This is expected since eme determines the timing of emergence, from when CC starts to accumulate. After emergence, other parameters begin to exert influence on CC, which substantially reduces the impact of eme. ccs and den are also very influential parameters at NE3 and Xiaotangshan from emergence, which is consistent with results from Jin et al. (2018). Other influential parameters depend on the site and scenario, and the parameters as well as their temporal behaviours are in general similar among scenarios at the same site. In maize modelling, ccx is the dominant parameter on CC from the leaf stage until before maturity at both NE3 and Monze. For winter wheat at Xiaotangshan, rtx and/or ccx have a large impact on CC during most of the growing season.

The sensitivity dynamics were also evaluated for crop biomass (Figure 7) during the growing season. The most influential parameters overlap with those on CC dynamics, as CC affects the amount of water transpired, which determines crop biomass generation. In addition, wp^* and wpy also have large impacts on crop biomass. Similar to the patterns shown in Figure 6, eme is the dominant factor on crop biomass at the beginning of the growing season for all site-crop-scenario combinations. As biomass is derived as the product of crop transpiration and wp^*, the influential parameters show some similarities with those on crop transpiration (Figure 5). For example, tb plays an important role on maize biomass at the NE3 site with increased sensitivity under wetter conditions, and *cgc* is only very influential for maize at the Monze site. However, while *ccx* is very influential on maize transpiration at the Monze site, it is not among the top 5 influential parameters on maize biomass. This is also in contrast with the analysis for CC, where *ccx* has a dominant effect on CC in the mid-season.

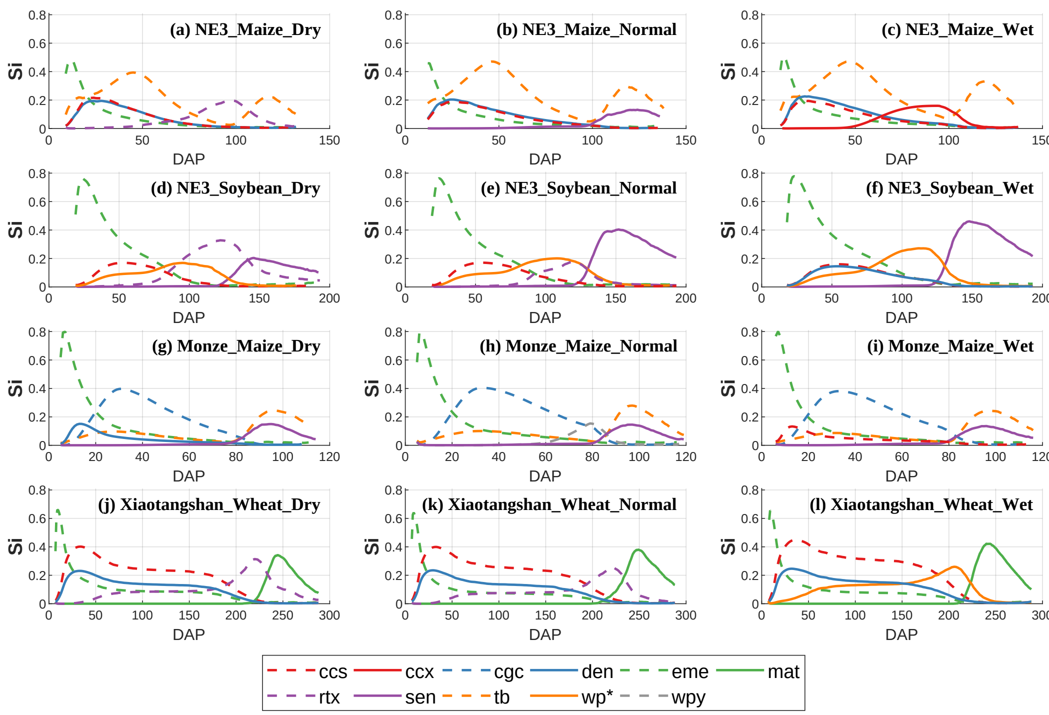

Figure 7: S_i time series of the five most influential factors on crop biomass throughout the growing season.

4. Discussion

4.1. Parameter Ranges

As a generic growth module is used for all crops in AquaCrop, the differences in sensitivity indices are essentially caused by the different parameter ranges used for different crops. For a given crop, the parameter ranges are known to have effects on the absolute sensitivity as well as the relative sensitivity rankings of all considered parameters (Wang et al., 2013). Recently, Jin et al. (2018) evaluated the influence of parameter variation by allowing different fluctuations in the parameter range, and demonstrated a clear impact on the parameter sensitivities. The determination of ranges is therefore critical for robust and trustworthy SA results (Punt and Hilborn, 1997; Shin et al., 2013; Wang et al., 2013). As the variation in each parameter is often non-uniform, the key is to use a range that is physically valid and locally reasonable.

The choice of parameter ranges is application-dependent, and the climatic and geophysical conditions of the study area should be considered. In this study, the parameter ranges for those with physical meaning were determined based on model documentation (Raes et al., 2018a,b,c) or previous studies over the chosen areas (Hou et al., 2014; Foolad et al., 2017; Ordonez et al., 2018; Thierfelder and Wall, 2009; Shan et al., 2019), such that they are valid in the environment of the application. For parameters with only a reference value (instead of a range) provided, the ranges were determined by allowing the parameters to vary within a range around the reference value, with consideration of the range width used for other crops. For parameters without physical meaning (e.g., shape and stress factors), the full plausible ranges of the parameter values in the model were adopted (Vanuytrecht et al., 2014b) to allow sufficient variations. In particular, as different hybrids/cultivars may be planted in different growing seasons, the full ranges of phenological parameters recommended in the model documentation were adopted. This is to ensure that the differences in crop development and responses to water stress among hybrids/cultivars are accounted for. The parameters were assumed to be uniformly distributed within the given ranges. The assumption of the parameter distribution has a smaller impact on the parameter sensitivity compared to the parameter ranges (Helton, 1993).

4.2. Influence of Target Output and Environmental Conditions

Crop yield is the most important output of all crop growth models, and naturally most parameter sensitivity studies have used crop yield as the target model output. Though crop yield is the final product of all growth processes and is therefore indirectly affected by the relevant parameters in the intermediate processes, the parameter sensitivities may not be the same when a different target output is used. Results from this study confirmed that the sensitivity magnitudes and influential parameter rankings were different for crop yield and transpiration. In particular, the parameters controlling biomass generation (e.g., wp^*, wpy) and yield formation (e.g., $hilen$) have no influence on the total transpiration. Despite the differences, some parameters affecting processes of root development (e.g., rtx, $root$), canopy development and senescence (e.g, ccx, sen) prove to have large impacts on both yield and transpiration under different scenarios. Given the fact that these processes are fundamental to crop growth, there is a large chance that those parameters would also be influential under similar conditions if other target outputs were used.

To account for the environmental influence on the sensitivity analysis, three scenarios featuring different wetness conditions were determined based on historical precipitation data. The results clearly demonstrated the substantial effect of the environmental conditions on the sensitivity analyses. The differences were most evident when the water stress variation among scenarios is large (e.g., at the NE3 site). At the Monze and Xiaotangshan sites, despite the large precipitation differences between scenarios, the water stress is either very high or very low under all scenarios, leading to similar analyses under different scenarios. This implies that water stress indices or other soil wetness indices may provide more direct information in distinguishing different scenarios than precipitation. Furthermore, the sensitivity differences among growing seasons under the same scenario (e.g., the dry and normal scenarios for maize at NE3) suggest that the temporal distribution of precipitation also plays an important role on the parameter sensitivities, which should be investigated further in future studies.

4.3. Influential / Non-influential Parameters: Implications for Model Implementation

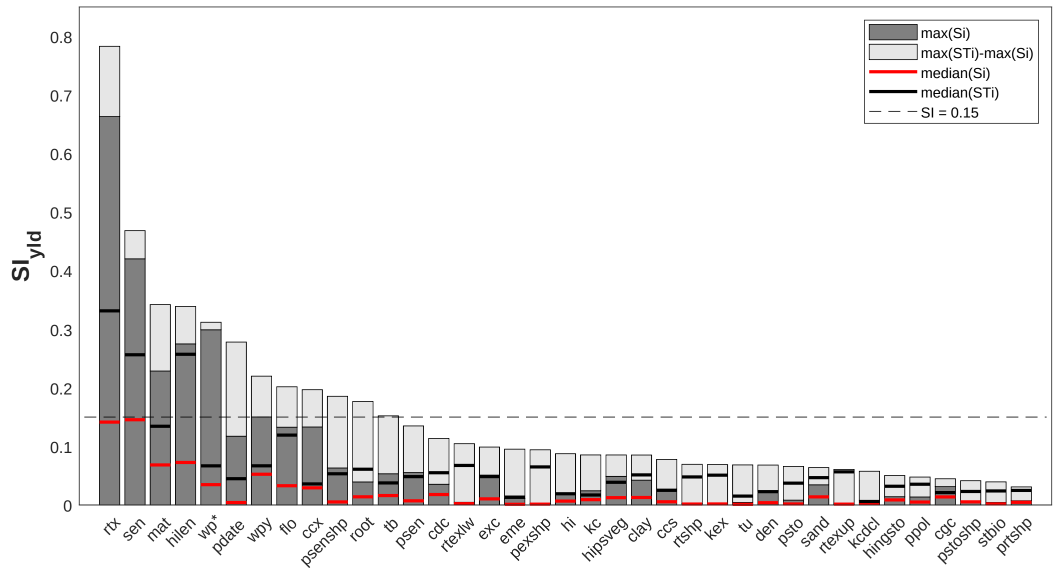

Figure 8: Maximum first-order (dark grey) sensitivity indices and interaction with other parameters (light grey) on crop yield across all site-crop-scenario conditions for all parameters evaluated using the EFAST method. The median values for S_i and ST_i are marked in thick red and black lines across the bars.

The apparent differences in parameter sensitivity rankings under different environmental conditions in this study indicate that it is impossible to derive a list of key parameters that is universally valid for all environmental conditions. Yet, the overlaps of influential parameter subsets under different site-crop-scenario combinations imply that some parameters may have large influences under diverse conditions, and that a summary of these parameters can serve as a guide for calibrating key model processes in other dryland environments. Similarly, some parameters prove to have little effect on the model outputs under all conditions evaluated, which provides a basis for potential model simplification.

Figure 8 shows the maximum S_i and ST_i using crop yield as the target variable for all the parameters evaluated using the EFAST method. A total of 84 EFAST evaluations (4 site-crop combinations * 3 scenarios * 7 growing seasons) were analysed. There are 37 parameters which were involved in the EFAST analysis at least once, and the magnitude and distribution of the sensitivity indices were markedly different. Following Vanuytrecht et al. (2014b), an arbitrary threshold of $ST_i = 0.15$ is used to distinguish between the influential and non-influential parameters. Three parameters $(rtx, sen, hilen)$ contribute to more than 15% of the crop yield variance (ST_i > 0.15) for more than half of the environmental conditions examined, and a few other parameters also have a large influence under certain conditions. The results highlight the importance of accurate parametrization of root and crop development variables, which was also demonstrated by previous studies in different regions (Pogson et al., 2012; Vanuytrecht et al., 2014b). Similarly, the parameter sensitivity indices on crop transpiration are shown in Figure 9. As can be seen, the parameters with significant influence on transpiration largely overlap with those derived for crop yield.

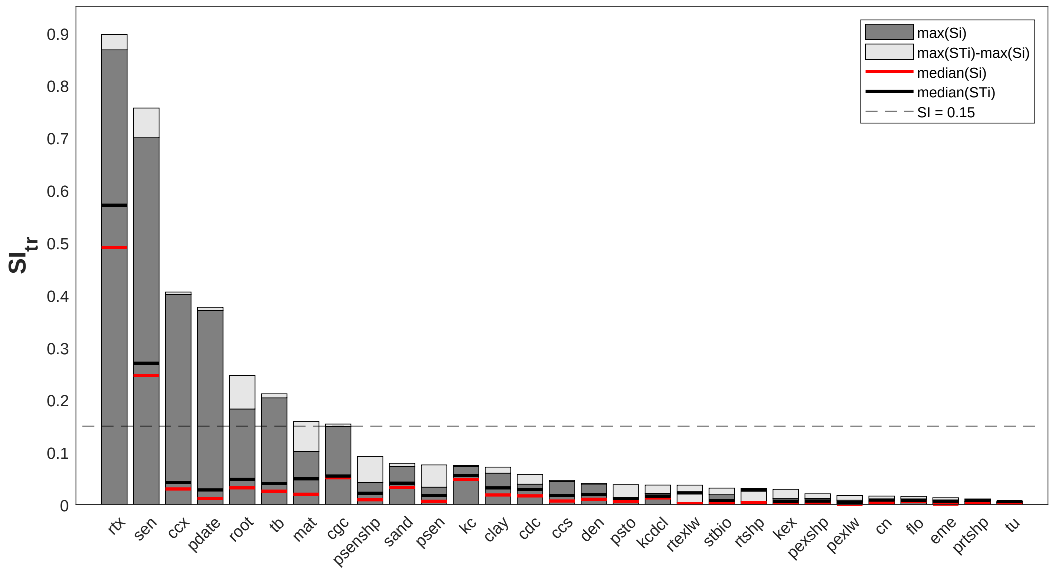

Figure 9: Maximum sensitivity indices on total transpiration using the EFAST method.

Crop models need to be calibrated before implementation, which requires expert knowledge and can be a time-consuming task. For example, an online survey suggests that the median time spent on crop model calibration is 25 days (Seidel et al., 2018). Prioritizing the calibration of a small subset of key parameters may substantially reduce the model parametrization workload for new applications. By synthesizing the EFAST results under different wetness conditions, the major influential parameters for the three crops are summarized under both high and low water stress (Table 3). Table 3 suggests that only a handful of parameters out of the 49 analyzed have large impacts on AquaCrop outputs. As such, calibration of these parameters should be prioritized in model implementation. In contrast, the majority of parameters not listed have no or negligible influence, which implies that these

Table 3: Major influential parameters of AquaCrop (v6.0) under high/low water stress for the three crops on yield and transpiration. The parameters are listed in alphabetical order.

Condition	**Crop**	**Yield**	**Transpiration**
Under High Water Stress	Maize	*hilen* *rtx* *sen*	*ccx* *root* *rtx* *sen*
	Soybean	*rtx* *wp**	*rtx*
	Winter Wheat	*mat* *pdate* *rtx*	*rtx*
Under Low Water Stress	Maize	*ccx* *flo* *hilen* *mat* *sen* *wpy*	*ccx* *cgc* *pdate* *sen* *tb*
	Soybean	*sen* *wp** *wpy*	*sen*
	Winter Wheat	*hilen* *mat* *sen* *wp**	*mat* *sen*

parameters may be given any value within their pre-defined ranges (e.g., the mid-value) without causing a large variation on the model outputs. Giving non-influential parameters fixed values may significantly reduce the time cost for calibration. For model developers, the large amount of parameters with no/negligible influence on model outputs also implies that there is room for model simplification for applications in dryland environments.

4.4. Sensitivity Dynamics: Implications for Data Assimilation

Similar to other numerical models in environmental science, crop models are vulnerable to uncertainties from three major sources: input data, model structure and parametrization (Liu and Gupta, 2007). Many studies have adopted data assimilation techniques to reduce simulation uncertainties. While most of the studies focused on updating model states using in situ or remote sensing observations (Li et al., 2014; Liu et al., 2016; Linker and Ioslovich, 2017; Silvestro et al., 2017a; Xie et al., 2017; Kang and Özdoğan, 2019; Jin et al., 2020), few have tried to update model parameters simultaneously (De Wit et al., 2012). Previous studies have assimilated canopy cover and/or biomass observations into the AquaCrop model to update the corresponding model states (Linker and Ioslovich, 2017; Silvestro et al., 2017a; Jin et al., 2020; Lu et al., 2021), but no parameter updates have been reported.

Joint state-parameter update (or the augmented-state data assimilation) should theoretically outperform state-only update, but is hampered by the limited knowledge on the optimal construction of the update vector. Our study used daily canopy cover and crop biomass simulations as the target variables, and demonstrated that the parameter influence on the crop states is stage-dependent. Here the main influence (S_i) instead of the total influence

(ST_i) was analysed in Figure 6 and 7, because a larger S_i would render the parameter more identifiable and retrievable through data assimilation (Saltelli et al., 2000b; Varella et al., 2010). For example, *ccx* can be updated by assimilating canopy cover observations in the mid-stage under the wet conditions, which may improve crop simulation since *ccx* has a significant influence on crop yield and transpiration (Table 3). Likewise, both biomass and canopy cover data may be used to update *sen* in the late growing season under some conditions, while canopy cover contains more information on *rtx* under higher water stress. Additionally, *eme* can be updated in the initial days of the growing season under all conditions, but the improvement on crop yield and transpiration may be marginal, since *eme* does not have a significant impact on the outputs. The results may thus serve as a reference for data assimilation studies with parameter updates using AquaCrop, and the sensitivity dynamics for other model states can also be derived.

4.5. Comparison with AquaCrop v5.0

The AquaCrop v6.0 model used in this study was released as an improved version of the previous AquaCrop v5.0. The major improvement involves an enhanced performance in very dry environments, including early-stage canopy development, root deepening in dry subsoil and water stress mitigation under light rain (FAO, 2017). To evaluate the differences in parameter sensitivities between the two versions, the entire experiment was rerun for AquaCrop v5.0. The five parameters with the largest difference in EFAST sensitivity indices are plotted in Figure 10 for crop yield and transpiration. The sensitivity indices from the two versions are comparable for most parameters, particularly when the crop is not severely water-stressed (e.g., at

Monze). This is expected since the improvement is mainly focused on crop simulation under dry conditions. A substantial difference is the reduced impact of clay content (*clay*) on both crop yield and transpiration, which is seen under most environmental conditions. *clay* affects crop growth via its impact on soil hydraulic properties, which influence soil water stress. In AquaCrop v6.0, the high water stress under the dry conditions is mitigated by (1) assuming the expansion rate of canopy cover is independent of soil moisture at the early phase of canopy cover development, and (2) comparing the depletion in the total root zone with the depletion of the top soil, which determines the part of the soil profile that is the wettest (FAO, 2017). As a result, the water stress under dry conditions becomes smaller, which leads to a reduced impact of *clay*. This suggests that the parameter sensitivities are also influenced by the model version, and that AquaCrop v6.0 tends to be more robust to uncertainties in soil properties.

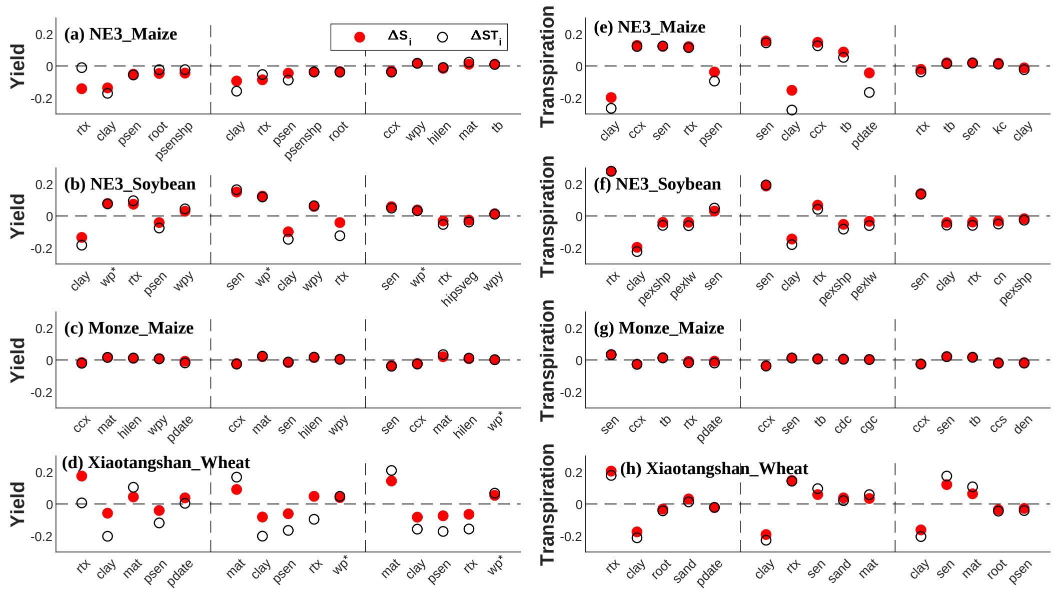

Figure 10: S_i and ST_i differences ($SI^{v6.0}$-$SI^{v5.0}$) between AquaCrop v6.0 and v5.0. Only the five parameters with the largest difference are plotted. The three scenarios are separated by the vertical dashed lines.

4.6. Transferability of Method and Results

A two-stage sensitivity analysis was adopted in this study to reduce the large computational time required for an EFAST-only analysis. For example, the runtime of an EFAST analysis for all the 49 parameters using a desktop computer (Intel i7-7700 CPU 3.6 GHz, 16 GB RAM) is around 88 hours (481,425 runs) under the same settings. When the non-influential parameters are filtered out, the runtime is reduced to between 13 and 52 hours. The runtime reduction is expected to be greater when the two-stage sensitivity analysis is applied to other more complex models. In contrast, the runtime of the Morris method is only 4.5 hours (25,000 runs). As the application of the Morris method is not computationally expensive and the results agree well with those from the EFAST method, it is suggested that a Morris sensitivity analysis should at least be performed under the local environmental condition before crop modelling.

Since water stress plays a key role in crop growth (particularly under dry conditions), the large impact of parameters relevant to crop water use (e.g., rtx, ccx) is also expected to be valid in other models that depict water stress on crop growth. For models based on light use efficiency such as STICS (Brisson et al., 1998), EPIC (Williams, 1990) and CERES (Jones and Kiniry, 1986), the parameters relevant to photosynthesis and radiation use may have a larger impact on model outputs (Campos et al., 2018; Li et al., 2019). The EFAST results from different growing seasons within one scenario imply that the temporal distribution of precipitation has an impact on the parameter sensitivities, which should be investigated further in future studies. Though many site-crop-scenario combinations were evaluated, this study is not exhaustive and other unconsidered environmental conditions may lead to different parameter sensitivity rankings. This study was mainly focused on the impact of parameters under various climatic conditions, and the impact of field management practices (e.g., irrigation, fertility stress) was not evaluated.

5. Conclusions

In this study, we performed a two-stage global sensitivity analysis of crop yield and transpiration for the FAO-AquaCrop model (version 6.0) in three dryland farming areas with different climatic conditions. A total of 49 parameters were evaluated for several staple crops (maize, soybean and winter wheat) using the Morris screening method and the variance-based EFAST method. Results from the two methods agree well, and show that only a handful of parameters have significant impact on crop yield and transpiration. The parameter sensitivities depend on the target model output and are affected by the wetness condition. Specifically, the parameters relevant to root development (e.g., *rtx*) tend to have large impacts under high water stress, while parameters controlling maximum canopy cover and senescence (e.g., *ccx*, *sen*) have considerable influence when the water stress is low. A day-by-day analysis of the parameter sensitivity dynamics of canopy cover and crop biomass suggests that the parameter sensitivity is stage-dependent. A further comparison with AquaCrop version 5.0 suggests that AquaCrop version 6.0 is less sensitive to uncertainties in soil properties. The analysis also implies that the temporal distribution of precipitation also affects parameter sensitivities, which should be investigated in future studies.

Acknowledgements

This work was partly funded through the 'A new paradigm in precision agriculture: assimilation of ultra-fine resolution data into a crop-yield forecasting model' project, supported by the King Abdullah University of Science and Technology, grant number OSR-2017-CRG6, and through the 'Building REsearch Capacity for sustainable water and food security In drylands of sub-saharan Africa (BRECcIA)' project, which is supported by UK Research and Innovation as part of the Global Challenges Research Fund, grant number NE/P021093/1. Matthew McCabe was funded by KAUST. G. De Lannoy was funded by EU project SHui GA 773903. The authors thank

Dr. Francesca Pianosi from University of Bristol for her help in performing the sensitivity analysis.

References

Adeboye, O.B., Schultz, B., Adekalu, K.O., Prasad, K.C., 2019. Performance evaluation of AquaCrop in simulating soil water storage, yield, and water productivity of rainfed soybeans (Glycine max L. merr) in Ile-Ife, Nigeria. Agricultural Water Management 213, 1130–1146.

Akumaga, U., Tarhule, A., Yusuf, A.A., 2017. Validation and testing of the FAO AquaCrop model under different levels of nitrogen fertilizer on rainfed maize in Nigeria, West Africa. Agricultural and Forest Meteorology 232, 225–234.

Allen, R., Pereira, L., Raes, D., Smith, M., 1998. Crop evapotranspiration: guidelines for computing crop water requirements. Irrigation and Drainage Paper 56, 300.

Bello, Z., Walker, S., 2017. Evaluating AquaCrop model for simulating production of amaranthus (Amaranthus cruentus) a leafy vegetable, under irrigation and rainfed conditions. Agricultural and Forest Meteorology 247, 300–310.

Brisson, N., Mary, B., Ripoche, D., Jeuffroy, M.H., Ruget, F., Nicoullaud, B., Gate, P., Devienne-Barret, F., Antonioletti, R., Durr, C., et al., 1998. STICS: a generic model for the simulation of crops and their water and nitrogen balances. I. Theory and parameterization applied to wheat and corn. Agronomie 18, 311–346.

Campolongo, F., Cariboni, J., Saltelli, A., 2007. An effective screening design for sensitivity analysis of large models. Environmental Modelling & Software 22, 1509–1518.

Campos, I., González-Gómez, L., Villodre, J., González-Piqueras, J., Suyker, A.E., Calera, A., 2018. Remote sensing-based crop biomass with water or light-driven crop growth models in wheat commercial fields. Field Crops Research 216, 175–188.

Cariboni, J., Gatelli, D., Liska, R., Saltelli, A., 2007. The role of sensitivity analysis in ecological modelling. Ecological Modelling 203, 167–182.

Chibarabada, T., Modi, A., Mabhaudhi, T., 2020. Calibration and evaluation of aquacrop for groundnut (Arachis hypogaea) under water deficit conditions. Agricultural and Forest Meteorology 281, 107850.

Confalonieri, R., Bellocchi, G., Bregaglio, S., Donatelli, M., Acutis, M., 2010a. Comparison of sensitivity analysis techniques: a case study with the rice model WARM. Ecological Modelling 221, 1897–1906.

Confalonieri, R., Bellocchi, G., Tarantola, S., Acutis, M., Donatelli, M., Genovese, G., 2010b. Sensitivity analysis of the rice model WARM in Europe: exploring the effects of different locations, climates and methods of analysis on model sensitivity to crop parameters. Environmental Modelling & Software 25, 479–488.

Cukier, R., Levine, H., Shuler, K., 1978. Nonlinear sensitivity analysis of multiparameter model systems. Journal of Computational Physics 26, 1–42.

De Wit, A., Duveiller, G., Defourny, P., 2012. Estimating regional winter wheat yield with WOFOST through the assimilation of green area index retrieved from MODIS observations. Agricultural and Forest Meteorology 164, 39–52.

Doorenbos, J., Kassam, A., 1979. Yield response to water. Irrigation and Drainage Paper 33, 257.

Fang, Y., Du, Y., Wang, J., Wu, A., Qiao, S., Xu, B., Zhang, S., Siddique, K.H., Chen, Y., 2017. Moderate drought stress affected root growth and grain yield in old, modern and newly released cultivars of winter wheat. Frontiers in Plant Science 8, 672.

FAO, 2017. Aquacrop update and new features: Version 6.0. Food and Agriculture Organization of the United Nations, Rome, Italy .

Foolad, F., Franz, T.E., Wang, T., Gibson, J., Kilic, A., Allen, R.G., Suyker, A., 2017. Feasibility analysis of using inverse modeling for estimating field-scale evapotranspiration in maize and soybean fields from soil water content monitoring networks. Hydrology and Earth System Sciences 21, 1263.

Foster, T., Brozović, N., Butler, A., Neale, C., Raes, D., Steduto, P., Fereres, E., Hsiao, T.C., 2017. AquaCrop-OS: An open source version of FAO's crop water productivity model. Agricultural Water Management 181, 18–22.

Guo, D., Zhao, R., Xing, X., Ma, X., 2019. Global sensitivity and uncertainty analysis of the AquaCrop model for maize under different irrigation and fertilizer management conditions. Archives of Agronomy and Soil Science , 1–19.

Helton, J.C., 1993. Uncertainty and sensitivity analysis techniques for use in performance assessment for radioactive waste disposal. Reliability Engineering & System Safety 42, 327–367.

Hou, P., Liu, Y., Xie, R., Ming, B., Ma, D., Li, S., Mei, X., 2014. Temporal and spatial variation in accumulated temperature requirements of maize. Field Crops Research 158, 55–64.

Hsiao, T.C., Heng, L., Steduto, P., Rojas-Lara, B., Raes, D., Fereres, E., 2009. AquaCrop-The FAO crop model to simulate yield response to water: III. Parameterization and testing for maize. Agronomy Journal 101, 448–459.

Huang, J., Yu, H., Guan, X., Wang, G., Guo, R., 2016. Accelerated dryland expansion under climate change. Nature Climate Change 6, 166.

Iooss, B., Lemaître, P., 2015. A review on global sensitivity analysis methods, in: Uncertainty management in simulation-optimization of complex systems. Springer, pp. 101–122.

Jin, X., Li, Z., Feng, H., Ren, Z., Li, S., 2020. Estimation of maize yield by assimilating biomass and canopy cover derived from hyperspectral data into the AquaCrop model. Agricultural Water Management 227, 105846.

Jin, X., Li, Z., Nie, C., Xu, X., Feng, H., Guo, W., Wang, J., 2018. Parameter sensitivity analysis of the AquaCrop model based on extended fourier amplitude sensitivity under different agro-meteorological conditions and application. Field Crops Research 226, 1–15.

Jones, C., Kiniry, J., 1986. CERES-Maize: A model of maize growth and development. Texas A&M Univer-sity Press, TX .

Kang, Y., Özdoğan, M., 2019. Field-level crop yield mapping with Landsat using a hierarchical data assimilation approach. Remote Sensing of Environment 228, 144–163.

Koevoets, I.T., Venema, J.H., Elzenga, J.T., Testerink, C., et al., 2016. Roots withstanding their environment: exploiting root system architecture responses to abiotic stress to improve crop tolerance. Frontiers in Plant Science 7, 1335.

Li, Y., Zhou, Q., Zhou, J., Zhang, G., Chen, C., Wang, J., 2014. Assimilating remote sensing information into a coupled hydrology-crop growth model to estimate regional maize yield in arid regions. Ecological Modelling 291, 15–27.

Li, Z.h., Jin, X.l., Liu, H.l., Xu, X.g., Wang, J.h., 2019. Global sensitivity analysis of wheat grain yield and quality and the related process variables from the DSSAT-CERES model based on the extended Fourier Amplitude Sensitivity Test method. Journal of Integrative Agriculture 18, 1547–1561.

Lin, B.B., 2010. The role of agroforestry in reducing water loss through soil evaporation and crop transpiration in coffee agroecosystems. Agricultural and Forest Meteorology 150, 510–518.

Linker, R., Ioslovich, I., 2017. Assimilation of canopy cover and biomass measurements in the crop model AquaCrop. Biosystems Engineering 162, 57–66.

Liu, J., Liu, Z., Zhu, A.X., Shen, F., Lei, Q., Duan, Z., 2019. Global sensitivity analysis of the APSIM-Oryza rice growth model under different environmental conditions. Science of the Total Environment 651, 953–968.

Liu, J., Zehnder, A.J., Yang, H., 2009. Global consumptive water use for crop production: The importance of green water and virtual water. Water Resources Research 45.

Liu, P.W., Bongiovanni, T., Monsivais-Huertero, A., Judge, J., Steele-Dunne, S., Bindlish, R., Jackson, T.J., 2016. Assimilation of active and passive microwave observations for improved estimates of soil moisture and crop growth. IEEE Journal of Selected Topics in Applied Earth Observations and Remote Sensing 9, 1357–1369.

Liu, Y., Gupta, H.V., 2007. Uncertainty in hydrologic modeling: Toward an integrated data assimilation framework. Water Resources Research 43.

Lu, Y., Chibarabada, T.P., Ziliani, M.G., Onema, J.M.K., McCabe, M.F., Sheffield, J., 2021. Assimilation of soil moisture and canopy cover data improves maize simulation using an under-calibrated crop model. Agricultural Water Management 252, 106884.

Mabhaudhi, T., Modi, A.T., Beletse, Y.G., 2014. Parameterisation and evaluation of the FAO-Aquacrop model for a South African taro (Colocasia esculenta L. schott) landrace. Agricultural and Forest Meteorology 192, 132–139.

Mbangiwa, N., Savage, M., Mabhaudhi, T., 2019. Modelling and measurement of water productivity and total evaporation in a dryland soybean crop. Agricultural and Forest Meteorology 266, 65–72.

Millennium Ecosystem Assessment, M., 2005. Ecosystems and human well-being. sythesis. Island Press Washington, DC .

Morris, M.D., 1991. Factorial sampling plans for preliminary computational experiments. Technometrics 33, 161–174.

Nossent, J., Elsen, P., Bauwens, W., 2011. Sobol' sensitivity analysis of a complex environmental model. Environmental Modelling & Software 26, 1515–1525.

Ordonez, R.A., Castellano, M.J., Hatfield, J.L., Helmers, M.J., Licht, M.A., Liebman, M., Dietzel, R., Martinez-Feria, R., Iqbal, J., Puntel, L.A., et al., 2018. Maize and soybean root front velocity and maximum depth in Iowa, USA. Field Crops Research 215, 122–131.

Pianosi, F., Beven, K., Freer, J., Hall, J.W., Rougier, J., Stephenson, D.B., Wagener, T., 2016. Sensitivity analysis of environmental models: A systematic review with practical workflow. Environmental Modelling & Software 79, 214–232.

Pianosi, F., Sarrazin, F., Wagener, T., 2015. A Matlab toolbox for global sensitivity analysis. Environmental Modelling & Software 70, 80–85.

Pogson, M., Hastings, A., Smith, P., 2012. Sensitivity of crop model predictions to entire meteorological and soil input datasets highlights vulnerability to drought. Environmental Modelling & Software 29, 37–43.

Punt, A.E., Hilborn, R., 1997. Fisheries stock assessment and decision analysis: the Bayesian approach. Reviews in Fish Biology and Fisheries 7, 35–63.

Qiu, R., Liu, C., Cui, N., Wu, Y., Wang, Z., Li, G., 2019. Evapotranspiration estimation using a modified Priestley-Taylor model in a rice-wheat rotation system. Agricultural Water Management 224, 105755.

Raes, D., Steduto, P., Hsiao, T., Fereres, E., 2018a. Aquacrop-The FAO crop model to simulate yield response to water: reference manual annexes. Food and Agriculture Organization of the United Nations. Rome, Italy .

Raes, D., Steduto, P., Hsiao, T., Fereres, E., 2018b. Aquacrop-The FAO crop model to simulate yield response to water: reference manual Chapter 2 - User guide. Food and Agriculture Organization of the United Nations. Rome, Italy .

Raes, D., Steduto, P., Hsiao, T., Fereres, E., 2018c. Aquacrop-The FAO crop model to simulate yield response to water: reference manual Chapter 3 - Calculation procedures. Food and Agriculture Organization of the United Nations. Rome, Italy .

Raes, D., Steduto, P., Hsiao, T.C., Fereres, E., 2009. AquaCrop-The FAO crop model to simulate yield response to water: II. Main algorithms and software description. Agronomy Journal 101, 438–447.

Ran, H., Kang, S., Hu, X., Li, S., Wang, W., Liu, F., 2020. Capability of a solar energy-driven crop model for simulating water consumption and yield of maize and its comparison with a water-driven crop model. Agricultural and Forest Meteorology 287, 107955.

Razavi, S., Gupta, H.V., 2015. What do we mean by sensitivity analysis? The need for comprehensive characterization of ”global” sensitivity in Earth and Environmental systems models. Water Resources Research 51, 3070–3092.

Reynolds, J.F., Smith, D.M.S., Lambin, E.F., Turner, B., Mortimore, M., Batterbury, S.P., Downing, T.E., Dowlatabadi, H., Fernández, R.J., Herrick, J.E., et al., 2007. Global desertification: building a science for dryland development. Science 316, 847–851.

Saltelli, A., Annoni, P., 2010. How to avoid a perfunctory sensitivity analysis. Environmental Modelling & Software 25, 1508–1517.

Saltelli, A., Chan, K., Scott, M., et al., 2000a. Sensitivity analysis. probability and statistics series. John and Wiley & Sons, New York .

Saltelli, A., Tarantola, S., Campolongo, F., et al., 2000b. Sensitivity anaysis as an ingredient of modeling. Statistical Science 15, 377–395.

Saltelli, A., Tarantola, S., Chan, K.S., 1999. A quantitative model-independent method for global sensitivity analysis of model output. Technometrics 41, 39–56.

Sandhu, R., Irmak, S., 2019a. Assessment of AquaCrop model in simulating maize canopy cover, soil-water, evapotranspiration, yield, and water productivity for different planting dates and densities under irrigated and rainfed conditions. Agricultural Water Management 224, 105753.

Sandhu, R., Irmak, S., 2019b. Performance of AquaCrop model in simulating maize growth, yield, and evapotranspiration under rainfed, limited and full irrigation. Agricultural Water Management 223, 105687.

Saxton, K.E., Rawls, W.J., 2006. Soil water characteristic estimates by texture and organic matter for hydrologic solutions. Soil Science Society of America Journal 70, 1569–1578.

Schlesinger, W.H., Jasechko, S., 2014. Transpiration in the global water cycle. Agricultural and Forest Meteorology 189, 115–117.

Seidel, S.J., Palosuo, T., Thorburn, P., Wallach, D., 2018. Towards improved calibration of crop models–Where are we now and where should we go? European Journal of Agronomy 94, 25–35.

Shan, G., Sun, Y., Zhou, H., Lammers, P.S., Grantz, D.A., Xue, X., Wang, Z., 2019. A horizontal mobile dielectric sensor to assess dynamic soil water content and flows: Direct measurements under drip irrigation compared with HYDRUS-2D model simulation. Biosystems Engineering 179, 13–21.

Sheffield, J., Goteti, G., Wood, E.F., 2006. Development of a 50-year high-resolution global dataset of meteorological forcings for land surface modeling. Journal of Climate 19, 3088–3111.

Shin, M.J., Guillaume, J.H., Croke, B.F., Jakeman, A.J., 2013. Addressing ten questions about conceptual rainfall–runoff models with global sensitivity analyses in R. Journal of Hydrology 503, 135–152.

Silvestro, P., Pignatti, S., Pascucci, S., Yang, H., Li, Z., Yang, G., Huang, W., Casa, R., 2017a. Estimating wheat yield in China at the field and district scale from the assimilation of satellite data into the Aquacrop and simple algorithm for yield (SAFY) models. Remote Sensing 9, 509.

Silvestro, P.C., Pignatti, S., Yang, H., Yang, G., Pascucci, S., Castaldi, F., Casa, R., 2017b. Sensitivity analysis of the Aquacrop and SAFYE crop models for the assessment of water limited winter wheat yield in regional scale applications. PloS One 12, e0187485.

Sobol, I.M., 1993. Sensitivity estimates for nonlinear mathematical models. Mathematical Modelling and Computational Experiments 1, 407–414.

Steduto, P., 2003. Biomass water-productivity. Comparing the growth-Engines of Crop Models. FAO expert consultation on crop water productivity under deficient water supply , 26–28.

Steduto, P., Hsiao, T.C., Fereres, E., 2007. On the conservative behavior of biomass water productivity. Irrigation Science 25, 189–207.

Steduto, P., Hsiao, T.C., Raes, D., Fereres, E., 2009. AquaCrop-The FAO crop model to simulate yield response to water: I. Concepts and underlying principles. Agronomy Journal 101, 426–437.

Thierfelder, C., Wall, P.C., 2009. Effects of conservation agriculture techniques on infiltration and soil water content in Zambia and Zimbabwe. Soil and Tillage Research 105, 217–227.

Vanuytrecht, E., Raes, D., Steduto, P., Hsiao, T.C., Fereres, E., Heng, L.K., Vila, M.G., Moreno, P.M., 2014a. AquaCrop: FAO's crop water productivity and yield response model. Environmental Modelling & Software 62, 351–360.

Vanuytrecht, E., Raes, D., Willems, P., 2014b. Global sensitivity analysis of yield output from the water productivity model. Environmental Modelling & Software 51, 323–332.

Varella, H., Guérif, M., Buis, S., 2010. Global sensitivity analysis measures the quality of parameter estimation: The case of soil parameters and a crop model. Environmental Modelling & Software 25, 310–319.

Verma, S.B., Dobermann, A., Cassman, K.G., Walters, D.T., Knops, J.M., Arkebauer, T.J., Suyker, A.E., Burba, G.G., Amos, B., Yang, H., et al., 2005. Annual carbon dioxide exchange in irrigated and rainfed maize-based agroecosystems. Agricultural and Forest Meteorology 131, 77–96.

Wang, J., Li, X., Lu, L., Fang, F., 2013. Parameter sensitivity analysis of crop growth models based on the extended Fourier Amplitude Sensitivity Test method. Environmental Modelling & Software 48, 171–182.

Wang, L., D'Odorico, P., Evans, J., Eldridge, D., McCabe, M., Caylor, K., King, E., 2012. Dryland ecohydrology and climate change: critical issues and technical advances. Hydrology and Earth System Sciences 16, 2585.

Wasaya, A., Zhang, X., Fang, Q., Yan, Z., 2018. Root phenotyping for drought tolerance: a review. Agronomy 8, 241.

Williams, I.N., Torn, M.S., 2015. Vegetation controls on surface heat flux partitioning, and land-atmosphere coupling. Geophysical Research Letters 42, 9416–9424.

Williams, J.R., 1990. The erosion-productivity impact calculator (EPIC) model: a case history. Philosophical Transactions of the Royal Society of London. Series B: Biological Sciences 329, 421–428.

Wu, M., Ran, Y., Jansson, P.E., Chen, P., Tan, X., Zhang, W., 2019. Global parameters sensitivity analysis of modeling water, energy and carbon exchange of an arid agricultural ecosystem. Agricultural and Forest Meteorology 271, 295–306.

Xie, Y., Wang, P., Bai, X., Khan, J., Zhang, S., Li, L., Wang, L., 2017. Assimilation of the leaf area index and vegetation temperature condition index for winter wheat yield estimation using Landsat imagery and the CERES-Wheat model. Agricultural and Forest Meteorology 246, 194–206.

Xu, J., Bai, W., Li, Y., Wang, H., Yang, S., Wei, Z., 2019. Modeling rice development and field water balance using AquaCrop model under drying-wetting cycle condition in eastern China. Agricultural Water Management 213, 289–297.